

# Nonplanar Ion Acoustic Waves in Electron-Ion Plasma with Generalized $(r, q)$ Distributed Electrons

Safder Hussain<sup>a</sup>, Muhammad Faisal<sup>a</sup> & Shakir Ullah<sup>a\*</sup>

<sup>a</sup>Department of Physics, Government Post Graduate College, Karak, KP 27200, Pakistan

Received: 18<sup>th</sup> April 2024; accepted: 10<sup>th</sup> July 2025

Standard reductive perturbation theory is used to analyze the motion of nonplanar ion acoustic waves in a plasma composed of cold ions and nonthermally distributed electrons. The nonplanar Korteweg de-Vries (KdV) equation is derived to describe the evolution of nonlinear nonplanar ion acoustic waves. It is discovered that the nonthermal electron parameters ( $r$  and  $q$ ) and the geometry factor ( $m$ ) have a considerable influence on the compressive and rarefactive ion-acoustic solitary wave characteristics. Because the wave profiles modify with  $r$ , the waves cannot be considered solitons. It is also discovered that the amplitudes of spherical ion acoustic waves are greater than those of cylindrical ion acoustic waves. The findings of this investigation contribute to our basic knowledge of the electron distribution function's full structure, including its high and low energy populations, as well as how nonplanar compressive and rarefactive ion acoustic waves develop in astrophysical and space plasmas.

**Keywords:** Generalized  $(r, q)$  velocity distribution, Reductive perturbation Method, Nonplanar Korteweg de-Vries (KdV) equation, Progressive wave solution, Compressive ion acoustic waves, Rarefactive ion acoustic waves

## 1 Introduction

Ion acoustic waves (IAWs), one of the fundamental wave phenomena of unmagnetized plasma, have been investigated both theoretically and experimentally for many years<sup>1</sup>. Stationary IAWs have been shown to occur as solitary or periodic waves. Due to quantitative variations between experiment and theory, the nonlinear ion-acoustic wave (IAW) theory has been developed to account for the consequences of a finite ion temperature<sup>2</sup>. Das and Nag studied how dynamics of nonlinear ion acoustic solitary wave (IASW) evolves in rotating plasma<sup>3</sup>. Paul and colleagues (2003) investigated ion acoustic solitons (IAS) in a multispecies plasma with warm positive ions, negative ions, and isothermal electrons<sup>4</sup>. Lonngren investigated the fundamental characteristics of IAS in an unmagnetized homogeneous plasma<sup>5</sup>. Deka and collaborators explored the features of the IASWs of dusty plasma in a laboratory<sup>6</sup>. The Maxwellian velocity distribution for particles is widely accepted as universally valid for macroscopic dynamical equilibrium systems. On the other hand, several observations of space plasmas are frequently identified by a particle velocity distribution function (VDF) with a high energy tail and may therefore

diverge from Maxwellian VDF<sup>7</sup>. Maxwellian VDF may be insufficient for describing systems with long-range interactions, such as gravitational and plasma systems, where unstable stationary states occur. The particles' energy distribution in the experiment for detecting IAWs may not be Maxwellian, making it difficult to calculate the proper particle temperature<sup>8</sup>. The non-Maxwellian VDFs of electrons in plasma were previously observed in experiments with a strong temperature gradient<sup>9</sup>. Plasma systems containing superthermal electrons are typically described by a long tail in the high energy region and flatness in the low energy region, deviating substantially from a Maxwellian VDF. Superthermality is caused by external forces operating on natural space environment plasmas or by wave particle interaction, which results in a  $(r, q)$ -like VDF<sup>10</sup>. The  $(r, q)$  velocity distribution approaches a Maxwellian distribution at  $r = 0$  and extremely large values of the spectral index  $q$ , however at low values of  $q$ , it exhibits a hard spectrum with a significant non-Maxwellian tail with a power law structure at high speed. Such a divergence in electron distribution substantially alters the circumstances for the formation of nonlinear structures like solitons, which are not observed in isothermal electron plasmas<sup>11</sup>.

\*Corresponding author: E-mail: shakirkhattak32@yahoo.com

The majority of these studies, however, are restricted to planar geometry. Nonplanar geometry would be more realistic in space and laboratory plasmas than planar geometry. There are auroral data that cannot be elucidated by a strictly planar geometry approach, especially at higher polar altitudes<sup>12</sup>. Williams and his colleagues experimentally discovered cylindrical and spherical solitons in electron-ion plasmas<sup>13</sup>. It's worth noting that nonplanar nonlinear waves have recently piqued the interest of many researchers<sup>14-20</sup>. The planar and nonplanar time-dependent dust-ion acoustic Gardner solitary waves were studied by Ghosh and associates in an unmagnetized dusty plasma consisting of nonextensive  $q$ -distributed electrons, positively and negatively charged dust, and Boltzmann distributed ions<sup>21</sup>. They investigated dynamics beyond of the KdV limit, where the typical nonlinear coefficient disappears. The findings reveal that the formation and properties of Gardner solitons are strongly influenced by the nonextensive electron distribution, especially in regions where KdV theory is no longer applicable. The properties of nonplanar ion-acoustic solitary waves in an unmagnetized, collisionless electron-positron-ion plasma with inertial ions and  $q$ -distributed electrons and positrons were investigated by Ghosh and associates<sup>22</sup>. The study indicates that the degree of particle nonextensivity has an enormous impact on rarefactive and compressive nonplanar Gardner solitons, demonstrating the substantial impact of the spectral index  $q$  in determining soliton features.

An effective analytical method for obtaining approximations of complex nonlinear partial differential equations that frequently occur in plasma physics is the Weighted Residual Method (WRM)<sup>23,24</sup>. WRM works especially well in the context of plasma to investigate nonlinear wave processes like ion-acoustic waves (IAWs) and ion-acoustic shock waves (IASWs), for which exact solutions are usually hard to obtain. WRM reduces the original problem to a simpler version by considering a suitable trial function that meets the boundary conditions and minimizing the residual, or the error from replacing the trial solution into the governing equation, in a weighted integral sense. Wave propagation properties through different plasma circumstances, such as nonplanar geometries, nonthermal particle distributions, and dissipative impacts, can be analyzed using this technique. Because of its adaptability and

effectiveness, WRM is a useful tool for mimicking wave dynamics in space and laboratory plasmas, giving insights on how physical parameters affect wave profile and evolution.

The motion of ion acoustic waves in an unmagnetized plasma in the presence of  $(r, q)$  distributed electrons and cold ions have not been documented in existing research to the best of the authors' knowledge. The main objectives of our current study are:

- i To explore the propagation features of ion-acoustic waves (IAWs) in a collisionless, unmagnetized plasma system made up of nonthermal electrons that follow a generalized  $(r, q)$ -distribution, which incorporates both low-energy core flatness as well as high-energy (suprathermal) tails and cold, inertial ions.
- ii To develop a theoretical framework that describes the nonlinear dynamics of ion-acoustic solitary waves (IASWs) in nonplanar geometries, namely spherical and cylindrical coordinate systems, where geometrical divergence dramatically changes the properties of wave propagation.
- iii To employ the reductive perturbation technique (RPT) for the derivation of the Korteweg-de Vries (KdV) equation, that dictates the evolution of small-amplitude nonlinear nonplanar IAWs in the plasma environment.
- iv To investigate how the spectral indices  $r$  and  $q$  play an exceptional role in the nonlinear and dispersive characteristics of the plasma medium, and to discover how alterations in these factors affect the width, amplitude, and polarity of the resulting IAWs profiles.
- v To solve the nonplanar KdV equation employing the Weighted Residual Method (WRM), an approximate analytical technique that enables effective study of wave structures in intricate geometries.
- vi To investigate the effects of different plasma variable values, such as the double spectral indices  $r$  and  $q$  and geometric curvature factors, on the width, amplitude, and polarity (compressive or rarefactive) of the resulting IAWs by numerically solving the derived solution of the KdV equation.
- vii To shed light on the ways in which nonlinear dispersive impacts, nonthermal electron density, and nonplanar geometry interact to influence the dynamics of IASWs. This will be useful in both

laboratory and astrophysical plasma settings where curvature and particle distributions differ from those found in classical models.

The remaining sections of the article is organized as follows. Section 2 offers the governing equations for our plasma model. The reductive perturbation approach is employed to get the KdV equation in Section 3. Section 4 covers numerical findings as well as analysis for solutions, while Section 5 is devoted to the conclusion.

**2 Fluid Model and Fundamental Governing Equations**

We're looking for cylindrical ion acoustic solitary waves (IASWs) in a collisionless, homogeneous, unmagnetized electron-ion (e-i) plasma made up of cold ions and nonthermal electrons with a generalized  $(r, q)$  distribution. The following set of equations govern the basic system of normalized equations in cylindrical geometry in such a plasma model<sup>25</sup>

$$\frac{\partial n_i}{\partial t} + \frac{\partial(n_i u_i)}{\partial \rho} + \frac{m}{\rho} n_i u_i = 0 \quad \dots (1)$$

$$\frac{\partial u_i}{\partial t} + u_i \frac{\partial u}{\partial \rho} + \frac{\partial \phi}{\partial \rho} = 0 \quad \dots (2)$$

Here  $n_i$  represents the number density of ions which is normalized by  $n_{i0}$  (equilibrium value number density of ions),  $\phi$  represents the electrostatic potential which is normalized by  $e\phi/kT_e$  where  $k_B$  is Boltzmann constant,  $e$  is the electronic charge and  $T_e$  is temperature of electron and  $u_i$  is the ion fluid's velocity which is normalized by the ion's acoustic velocity  $C_s (= \sqrt{k_B T_e / m_i})$ . The electrostatic potential  $\phi$  is calculated using the well-known Poisson's equation, which is given by

$$\frac{\partial^2 \phi}{\partial \rho^2} + \frac{m}{\rho} \frac{\partial \phi}{\partial \rho} (n_e - n_i) = 0 \quad \dots (3)$$

The subscripts  $e$  and  $i$  in the above expressions represent electron and ion, respectively.  $\rho$  is the radial coordinate, and  $u_i$  is the ion fluid's velocity in the  $\rho$  direction. Space and Time parameters are normalized by the Debye length  $\lambda_D = (k_B T_e / 4\pi n_{i0} e^2)^{1/2}$  and the inverse ion plasma frequency  $\omega_{pi}^{-1} = (4\pi n_{i0} e^2 / m_i)^{-1/2}$ , respectively. The electrons are taken to be  $(r, q)$  distributed, and the generalized  $(r, q)$  velocity distribution function for them is given by<sup>10</sup>

$$f_{(r,q)}(v) = N \left[ 1 + \frac{1}{q-1} \left( \frac{v^2 - 2e\phi/m_e}{\beta v_{th}^2} \right)^{r+1} \right]^{-q} \quad \dots (4)$$

Here

$$N = \frac{3\Gamma[q](q-1)^{-3/(2+2r)}}{4\pi\beta^{3/2}v_{th}^{3/2}\Gamma\left[q-\frac{3}{2+2r}\right]\Gamma\left[1+\frac{3}{2+2r}\right]} \quad \dots (5)$$

$$\beta = \frac{3(q-1)^{-1/(1+r)}\Gamma\left[q-\frac{3}{2+2r}\right]\Gamma\left[\frac{3}{2+2r}\right]}{2\Gamma\left[q-\frac{5}{2+2r}\right]\Gamma\left[\frac{5}{2+2r}\right]} \quad \dots (6)$$

By means of the cylindrical coordinates and after doing the integration over velocity space the electron's number density from Eq. (4) is found as<sup>26</sup>

$$n_e = 1 + A\phi + B\phi^2 + C\phi^3 \quad \dots (7)$$

where

$$A = \frac{(q-1)^{-1/(1+r)}\Gamma\left[q-\frac{1}{2+2r}\right]\Gamma\left[\frac{1}{2+2r}\right]}{2\beta\Gamma\left[\frac{3}{2+2r}\right]\Gamma\left[q-\frac{3}{2+2r}\right]} \quad \dots (8)$$

$$B = \frac{-(q-1)^{-2/(1+r)}\Gamma\left[q+\frac{1}{2+2r}\right]\Gamma\left[\frac{-1}{2+2r}\right]}{8\beta^2\Gamma\left[q-\frac{3}{2+2r}\right]\Gamma\left[\frac{3}{2+2r}\right]} \quad \dots (9)$$

$$C = \frac{(q-1)^{-3/(1+r)}\Gamma\left[q+\frac{3}{2+2r}\right]\Gamma\left[\frac{-3}{2+2r}\right]}{16\beta^3\Gamma\left[q-\frac{3}{2+2r}\right]\Gamma\left[\frac{3}{2+2r}\right]} \quad \dots (10)$$

It is pertinent to mention that the spectral indices  $r$  and  $q$  fulfill the conditions  $q(1+r) > 5/2$  and  $q > 1$ <sup>26</sup>. The generalized  $(r, q)$  distribution is reduced to Maxwellian distribution function when  $r = 0$  and  $q \rightarrow \infty$ , and to kappa distribution function when  $r = 0$  and  $q \rightarrow \kappa$ .

**3 Reductive Perturbation Technique and Derivation of the Nonplanar KdV Equation**

We examine the motion of small-amplitude ion acoustic solitary waves using the standard reductive perturbation method<sup>27</sup>. For this purpose, we introduce the following stretched coordinates

$$\xi = \epsilon^{1/2}(\rho - v_p t) \text{ and } \tau = \epsilon^{3/2} t \quad \dots (11)$$

Here  $v_p$  is the phase velocity of IAWs (ion acoustic waves) determined by the compatibility condition and  $\epsilon$  is a tiny expansion parameter ( $0 < \epsilon < 1$ ) that measures the perturbation's strength. In order to investigate the effects of propagation on nonplanar IAWs, we consider that all perturbed parameters are expanded as

$$\begin{pmatrix} n_i \\ u_i \\ \phi \end{pmatrix} = \begin{pmatrix} 1 \\ 0 \\ 0 \end{pmatrix} + \sum_{l=1}^{\infty} \epsilon^l \begin{pmatrix} n_i(\zeta, \eta, \tau) \\ u_i(\zeta, \eta, \tau) \\ \phi_l(\zeta, \eta, \tau) \end{pmatrix} \quad \dots (12)$$

We obtain the reduced expressions by incorporating Eq (12) into Eqs. (1-3) and gathering the different powers of  $\epsilon$ . We derive the following first order expressions for the lowest order in  $\epsilon$

$$n_1 = \frac{u_1}{v_p}, u_1 = \frac{\phi_1}{v_p}, \phi_1 = \frac{n_1}{A} \quad \dots (13)$$

Algebraic adjustments of the preceding equations result in the phase velocity equation shown below

$$v_p = \frac{1}{\sqrt{A}} \quad \dots (14)$$

We get the following set of expressions for the next higher order in  $\epsilon$

$$\begin{aligned} -v_p \partial_\xi n_2 + \partial_\xi u_2 + \partial_\tau n_1 + \partial_\xi n_1 u_1 + \frac{m u_1}{\lambda \tau} &= 0, \\ -v_p \partial_\xi u_2 + \partial_\tau u_1 + u_1 \partial_\xi u_1 + \partial_\xi \phi_1 &= 0 \quad \dots (15) \\ \partial_{\xi\xi} \phi_1 - A \phi_2 - B \phi_1^2 + n_2 &= 0. \end{aligned}$$

We derive the following expression in terms of  $\phi_1$  by algebraically manipulating Eqs (13-15)

$$\partial_\tau \phi_1 + \frac{m}{2\tau} \phi_1 + M_1 \phi_1 \partial_\xi \phi_1 + M_2 \partial_{\xi\xi\xi} \phi_1 = 0 \quad \dots (16)$$

The above equation is the nonplanar Korteweg de-Vries (KdV) equation with

$$M_1 = \frac{3}{2\lambda^2} - \lambda^3 B \quad \dots (17)$$

$$M_2 = \frac{\lambda^3}{2} \quad \dots (18)$$

Here  $M_1$  and  $M_2$  are the nonlinear and dispersion coefficients. One can also see that the nonlinear and the dispersion coefficients depends on the parameters  $r$  and  $q$ . Thus, we hope that  $r$  and  $q$  would modify the

dynamics of the nonlinear ion acoustic waves (NIAWs). The progressive wave solution of Eq (16) is given by (see appendix for complete detail and calculation)

$$\begin{aligned} \phi(\xi, \tau) &= a_0 \left(\frac{\tau}{\tau_0}\right)^{-\left(\frac{2m}{3}\right)} \sec h^2 \eta, \\ \eta &= \left(\frac{a_0 M_1}{12 R_2}\right)^{1/2} \left(\frac{\tau}{\tau_0}\right)^{-\left(\frac{m}{3}\right)} \left\{ \xi - \left(\frac{a_0 M_1 \tau_0}{3}\right) \left[ 1 + \frac{3}{3-2m} \left[ \left(\frac{\tau}{\tau_0}\right)^{\left(1-\frac{2m}{3}\right)} - 1 \right] \right] \right\} \quad \dots (19) \end{aligned}$$

where  $\tau_0$  indicates initial time scale or a reference time and  $a_0$  is the initial amplitude of the wave at  $\tau_0$ .

### 4 Results

In this part of the article, we will offer a numerical analysis of the solution to illustrate the analytical outcomes. To that end, we will look into the solution of the KdV equation. In this scenario, the IAW's nature is determined by the sign of the coefficient  $M_1$ , i.e., when  $M_1 > 0$  ( $M_1 < 0$ ), the wave is called compressive (rarefactive) IAW. Here, we will only explain compressive IAWs and similar explanation is valid for rarefactive IAWs.

Figure 1 illustrates the changes in the shape of the wave patterns for the cylindrical ( $m = 1$ ) ion acoustic waves and spherical ( $m = 2$ ) ion acoustic waves for  $\tau_0 = 13$  and different values of the spatial ( $\xi$ ) and time ( $\tau$ ) coordinates. As demonstrated in the plots, the IAWs' amplitude decreases as the time variable  $\tau$  increases. Because the IAWs' amplitude alters with time, progressive waves in nonplanar geometries cannot be regarded as solitons that preserve their shapes<sup>25</sup>. The diversity in the waveforms of spherical IAWs is likewise observed to be significantly greater than that of cylindrical IAWs. Furthermore, a spherical IAW has a greater amplitude than a cylindrical IAW.

Figure 2 depicts the IAWs for different values of spectral parameter  $q$  in cylindrical and in spherical

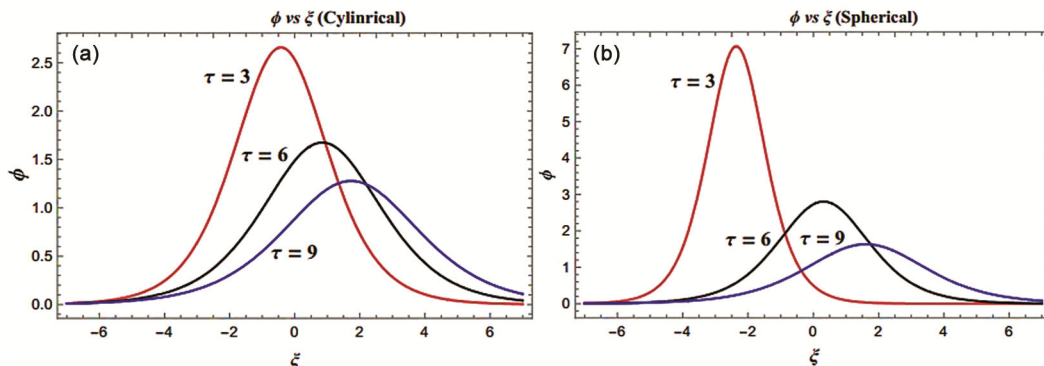


Fig. 1 — Wave profile variation for the cylindrical ( $m = 1$ ) and spherical ( $m = 2$ ) nonplanar KdV equations with  $a_0 = 1$ ,  $\tau_0 = 13$ ,  $\tau = 3, 6, 9$ ,  $r = 1$ , and  $q = 2$

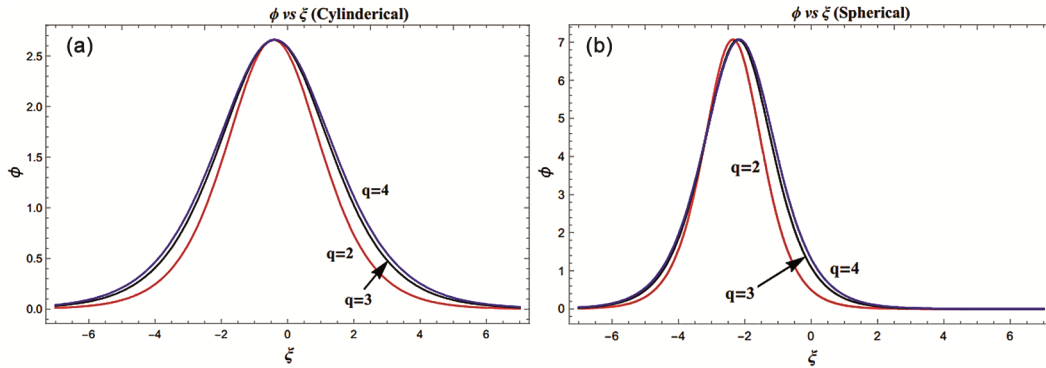


Fig. 2 — Wave profile variation for the cylindrical ( $m = 1$ ) and spherical ( $m = 2$ ) nonplanar KdV equations with  $a_0 = 1$ ,  $\tau_0 = 13$ ,  $\tau = 3$ ,  $r = 1$ , and  $q = 2, 3, 4$

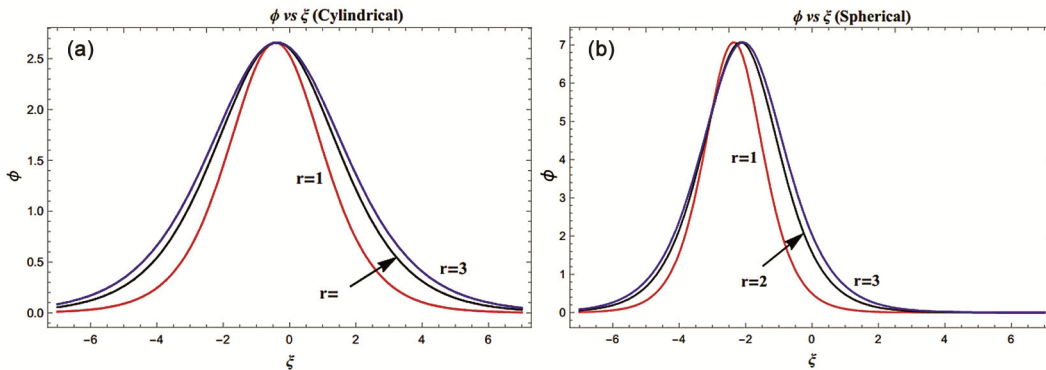


Fig. 3 — Wave profile variation for the cylindrical ( $m = 1$ ) and spherical ( $m = 2$ ) nonplanar KdV equations with  $a_0 = 1$ ,  $\tau_0 = 13$ ,  $\tau = 3$ ,  $r = 1, 2, 3$ , and  $q = 2$

geometries while keeping other plasma variables constant. It is seen that the width of IAWs enhances as  $q$  increases, implying that the concentration of electrons at high energy increases. It is pertinent to note that amplitude of the IAW is directly proportional to its velocity. As a result, the amplitude of spherical solitary IAWs is greater than that of cylindrical IAWs, indicating that they move faster.

Figure 3 depicts the effect of the spectral index  $r$  (the flatness of the distribution) on nonlinear IAWs. Figure 3 indicates that enhancing the electron population at low energy in low phase space density increases the width of the IAW while maintaining the other plasma parameters fixed. As previously stated, the amplitude of spherical IAWs is greater than that of cylindrical IAWs. It could be interesting to investigate the impacts of the double spectral indices  $r$  and  $q$  on some wave properties. As previously stated, the coefficients  $M_1$  and  $M_2$  are functions of double spectral indices  $r$  and  $q$ .

Figure 4 depicts the variations of nonlinear term coefficient  $M_1$  with the spectral indices  $q$  for various values of  $r$ . It is observed that the coefficient  $M_1$

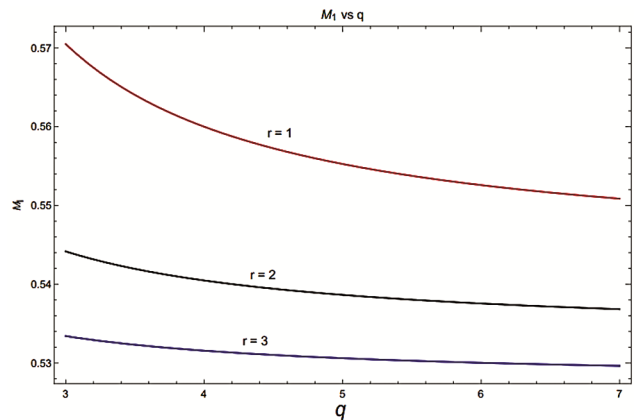


Fig. 4 — Nonlinearity coefficient variation ( $M_1$ ) with  $q$  for different values of  $r$

decreases when the population of electrons at low energies in high phase space density (flatness spectral index  $r$ ) increases. This system is capable of supporting compressive solitons.

Figure 5 shows how the nonlinear term coefficient  $M_1$  varies with the spectral indices  $r$  for different values of  $q$ . It is seen that when the population of electrons at high energies in low phase space density

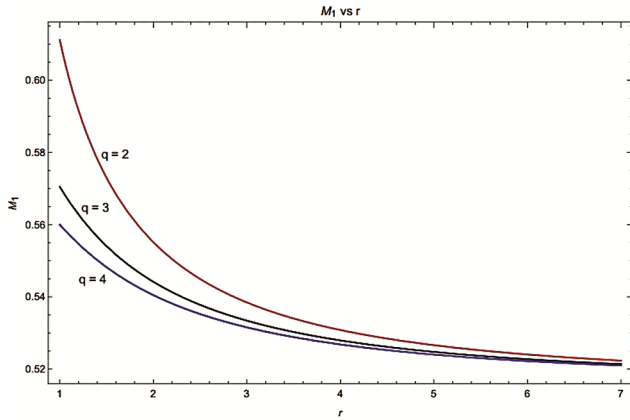


Fig. 5 — Nonlinearity coefficient variation ( $M_1$ ) with  $r$  for different values of  $q$

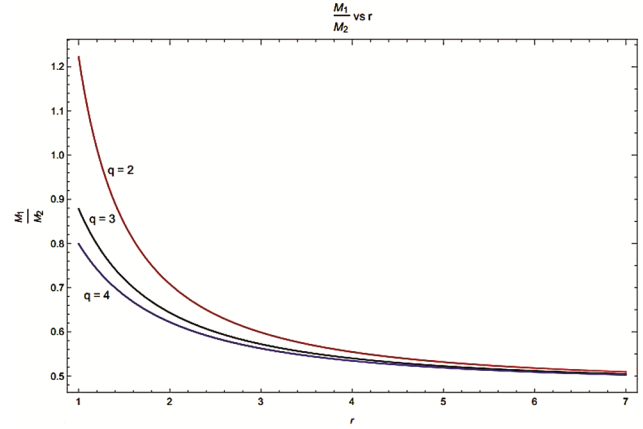


Fig. 7 — Steepening parameter variation ( $M_1/M_2$ ) with  $r$  for different values of  $q$

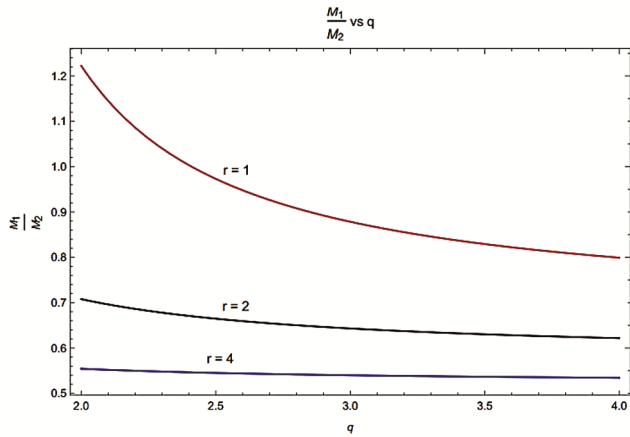


Fig. 6 — Steepening parameter variation ( $M_1/M_2$ ) with  $q$  for different values of  $r$

(tail spectral index  $q$ ) increases, the nonlinear coefficient  $M_1$  decreases. Additionally, this can support compressive solitons. Fig. 5. Nonlinearity coefficient variation ( $M_1$ ) with  $r$  for different values of  $q$ .

Another essential feature of solitary waves is their steepening effect (or bandwidth), which is related to the  $M_1/M_2$  ratio. This ratio is expected to be affected by the double spectral indices  $r$  and  $q$ . Figure 6 depicts the alterations of this ratio with  $q$  for various values of  $r$ . It is found that increasing the parameter  $r$  (population of electrons at low energies in high phase space density) flattens the waves while decreasing the spectral index  $r$  steepens them.

Figure 7 demonstrates the changes in this ratio with spectral index  $r$  for different values of spectral index  $q$ . It is discovered that increasing the parameter  $r$  (population of electrons at high energies in low phase space density) steepens the waves while decreasing the spectral index  $q$  flattens them.

Figure 8 demonstrates the rarefactive ion-acoustic waves (IAWs) dictated by the nonplanar Korteweg–de Vries (KdV) equation, where the electrostatic potential  $\phi$  has negative amplitudes, in comparison to the positive amplitudes seen in compressive IAWs. The entire wave dynamics remain consistent with those previously described for compressive profiles, including the impacts of nonlinearity, dispersion, and geometric curvature. The only essential difference lies in the polarity of the wave: compressive IAWs correspond to ion density enhancements and positive potential, while rarefactive IAWs are associated with regions of reduced ion density and negative potential. Similar to compressive waves, rarefactive IAWs widen as their amplitude declines with enhancing geometrical curvature because of increased geometric divergence. Rarefactive IAWs are therefore formed and propagated by the same physical processes as compressive ones, with the only difference being the polarity of the electrostatic disturbance.

The 3D time evolution of nonplanar compressive and rarefactive ion-acoustic waves (IAWs) is depicted in Figs 9 and 10, respectively. These graphs show how the electrostatic potential  $\phi(\xi, \tau)$  and its amplitude and spatial structure alter as time passes in spherical and cylindrical geometries. Because of geometric divergence, the positive potential profiles for nonplanar compressive IAWs (Figure 9) widen and get lower in height over time.

The potential dips for nonplanar rarefactive IAWs (Fig. 10) deepen and widen in a similar way demonstrating mirror-symmetric polarity behavior yet subject to the same underlying dynamics. The combined impacts of dispersion, curvature, and nonlinearity on the distortion and decay of solitary

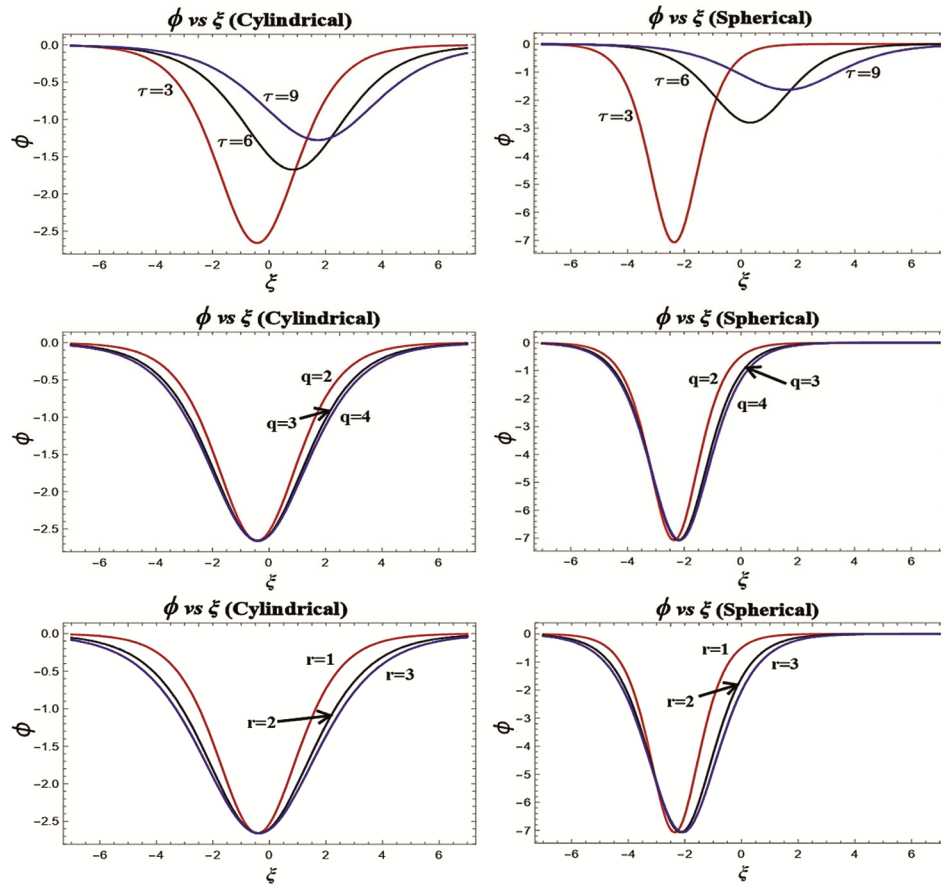


Fig. 8 — Rarefactive ion acoustic waves

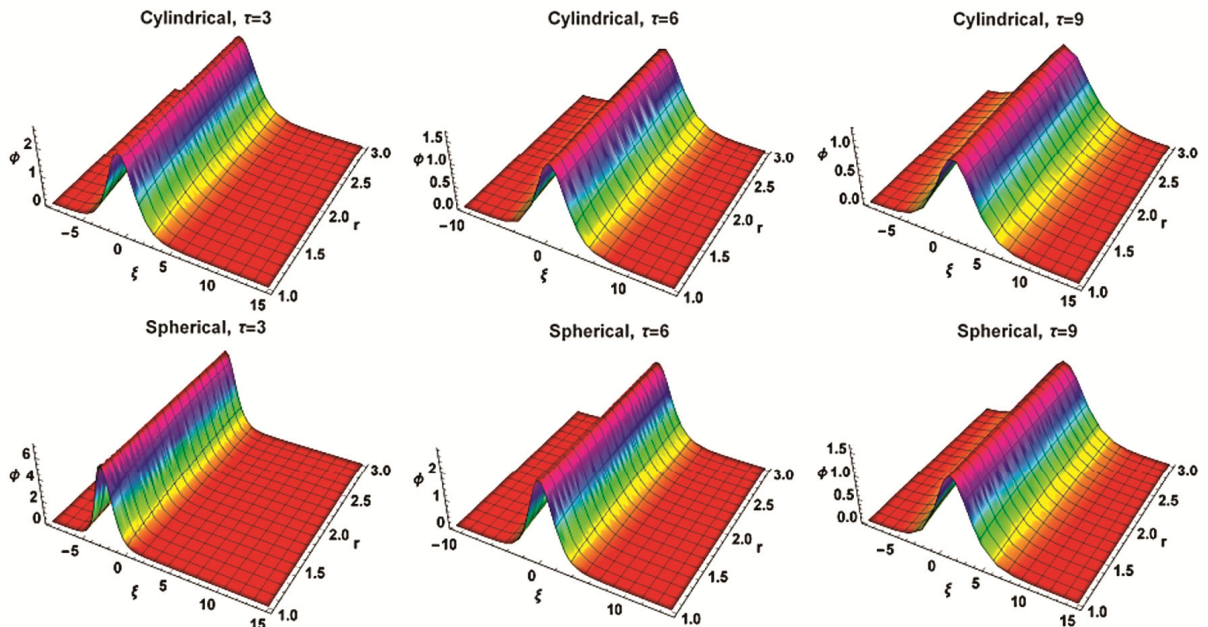


Fig. 9 — 3D time evolution of nonplanar Compressive ion-acoustic waves

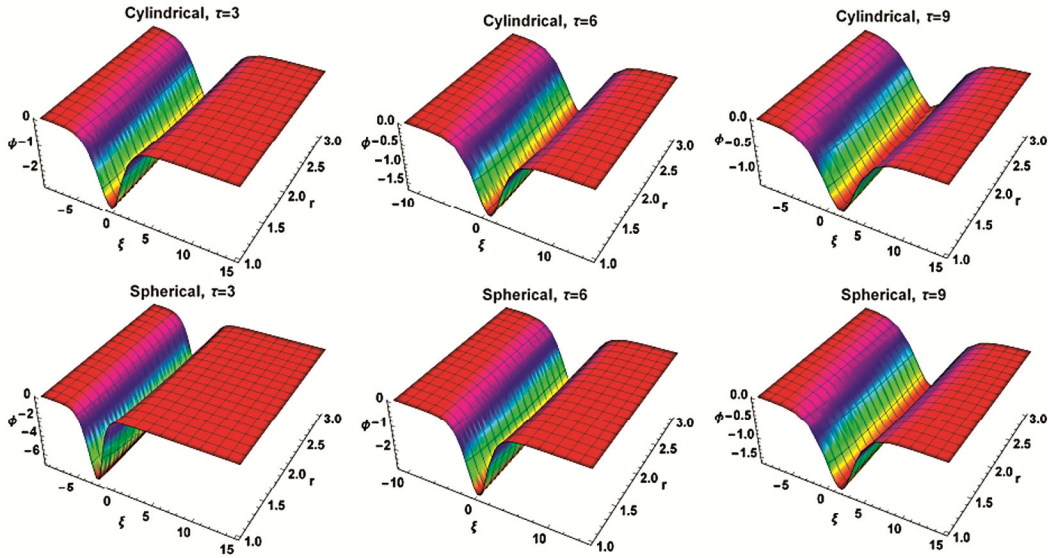


Fig. 10 — 3D time evolution of nonplanar Rarefactive ion-acoustic waves

wave profiles in nonplanar plasma environments are evident in both figures.

**5 Conclusion**

We investigated the nonlinear evolution of ion acoustic waves in an electron-ion plasma with  $(r, q)$  distributed electrons for the first time in order to discover the significance as well as relevance of the complete distribution profile in nonplanar geometries. Our results are based on a generalized and electron distribution with a flat top and at low energies superthermal tails at high energy. We used the standard reductive perturbation approach to obtain the nonplanar KdV equation for this purpose, which was subsequently employed to investigate the propagation features of IAWs based on the distribution profile by altering the corresponding values of the double spectral indices  $r$  and  $q$ . The amplitude of the IAWs has been seen to alter as the time parameter  $\tau$  is changed. According to the numerical analysis, as the time parameter  $\tau$  increases, the amplitudes of these nonplanar IAWs decrease. Because the wave profiles change with  $\tau$ , the waves are not considered solitons. It has been discovered that increasing the values of  $r$  and  $q$  widens the IAWs and vice versa. It is also discovered that the amplitudes of spherical IAWs are greater than those of cylindrical IAWs.

As a final remark, this investigation is likely to aid in understanding the nature of nonlinear excitation in the laboratory as well as astrophysical plasmas, where nonthermal electrons and ions are present.

**Appendix**

**Appendix A: Progressive Wave Solution**

In this section of the article, we will attempt to employ the modified weighted residual method to provide an approximate analytical solution for the nonplanar KdV Eq (16). Researchers have given many numerical solutions for such problems. Our obtained nonplanar evolution Eq (16) can be expressed in general form as

$$\partial_\tau W + \frac{m}{2\tau} W + \kappa_1 W \partial_\xi W + \kappa_2 \partial_{\xi\xi\xi} W = 0 \quad \dots (A1)$$

where the nonlinearity and dispersion coefficients are denoted by  $\kappa_1$  and  $\kappa_2$ , accordingly. When  $m = 0$  in the planar case and  $W = W_0$ , the evolution Eq. (A1) turns into

$$\partial_\tau W_0 + \kappa_1 W_0 \partial_\xi W_0 + \kappa_2 \partial_{\xi\xi\xi} W_0 = 0 \quad \dots (A2)$$

which is ordinary KdV equation. The evolution equation (A20) may be regarded as the limiting case of equation (A1), where the ratio  $(mW/2\tau)$  can be insignificant, when  $\tau$  is very large, that is,  $\tau > \tau_0$ . Therefore, the solitary wave solution of evolution expression (A2) may look like this

$$W_0(\xi, \tau) = a_0 \operatorname{sech}^2 \eta_0 \quad \dots (A3)$$

where  $\eta_0 = b_0(\xi - v_0\tau)$  and  $a_0$  is the fixed wave amplitude.  $b_0$  and  $v_0$  are given by

$$b_0 = \sqrt{\frac{a_0 \kappa_1}{12 \kappa_2}}, v_0 = \frac{a_0 \kappa_1}{3} \quad \dots (A4)$$

Based on the solution in Eq. (A3) we will suggest the following kind of solution for Eq. (A1)

$$W(\xi, \tau) = a(\tau) \sec h^2 \eta \quad \dots (A5)$$

where  $\eta = b(\tau)(\xi - v(\tau))$  and the unknown variables  $a(\tau)$ ,  $b(\tau)$  and  $v(\tau)$  are expressed as

$$b(\tau) = \sqrt{\frac{a(\tau)\kappa_1}{12\kappa_2}}, \frac{\partial v(\tau)}{\partial \tau} = \frac{a(\tau)\kappa_1}{3} \quad \dots (A6)$$

It is noted that Eqs. (A4) and (A6), are formally equivalents. After considering the equations (A6) and substituting Eq. (A5) into Eq. (A1) the residual term is as follows

$$R(\eta, \tau) = \left( \left[ \frac{\frac{\partial a(\tau)}{\partial \tau}}{a(\tau)} + \frac{m}{2\tau} \right] - \frac{\frac{\partial a(\tau)}{\partial \tau}}{b(\tau)} \eta \tanh \eta \right) \text{sech}^2 \eta \quad \dots (A7)$$

Because the expression in (A5) is not an exact solution to Eq. (A1), the residue factor  $R(\eta, \tau)$  cannot equal zero. After multiplying the residue factor  $R(\eta, \tau)$  by a weighting function, the result will be integrated with regard to  $\eta$ , from  $\eta = -\infty$  to  $\eta = \infty$ , with zero as the final result. This method was modeled after the weighted residual method, which is commonly used in applied mathematics. The present investigation provides the following equation by using the previously stated method and using  $\text{sech}^2 \eta$  as the weighting function

$$\left( \frac{\frac{\partial a(\tau)}{\partial \tau}}{a(\tau)} + \frac{m}{2\tau} \right) \int_{-\infty}^{\infty} \text{sech}^4 \eta d\eta = 0 \quad \dots (A8)$$

For  $a(\tau)$ , the following ordinary differential equation can be obtained as the integral  $\int_{-\infty}^{\infty} \text{sech}^4 \eta d\eta \neq 0$

$$\left( \frac{\frac{\partial a(\tau)}{\partial \tau}}{a(\tau)} + \frac{m}{2\tau} \right) = 0 \quad \dots (A9)$$

The following is the solution to this ordinary differential equation

$$a(\tau) = a_0 \left( \frac{\tau}{\tau_0} \right)^{-\frac{2m}{3}}, a(\tau) = b_0 \left( \frac{\tau}{\tau_0} \right)^{-\frac{m}{3}} \quad \dots (A10)$$

So,  $v(\tau)$  becomes

$$v(\tau) = v_0 \tau_0 \left( 1 - \frac{3}{3-2m} \left[ \left( \frac{\tau}{\tau_0} \right)^{\left( 1 - \frac{2m}{3} \right)} - 1 \right] \right) \quad \dots (A11)$$

In the present scenario,  $a_0$  is fixed and  $\tau_0$  is time factor ensuring that for  $\tau_0 < \tau$  ratio  $(mW/2\tau)$  can be

ignored. Therefore, the approximate analytical solution for the generalized nonplanar KdV equation can be expressed by

$$W(\xi, \tau) = a_0 \left( \frac{\tau}{\tau_0} \right)^{-\frac{2m}{3}} \sec h^2 \eta \quad \dots (A12)$$

and here

$$\eta = b(\tau)(\xi - v(\tau)) = b_0 \left( \frac{\tau}{\tau_0} \right)^{-\frac{m}{3}} \left( \xi - v_0 \tau_0 \left( 1 - \frac{33-2m\tau\tau_0}{1-2m3-1} \right) \right) \quad \dots (A13)$$

The velocity of propagation can be measured using

$$v(\tau) = v_0 \left( \frac{\tau}{\tau_0} \right)^{-\frac{2m}{3}} \quad \dots (A14)$$

The solutions in Eqs. (A10) - (A14) reduce to those in (A3) and (A4), considering  $m = 0$ . The nonplanar KdV equation (16) can be analytically approximated using the general form by selecting the variables  $\kappa_1$  and  $\kappa_2$  as follows: considering  $\phi_1 = \phi$ ,  $\kappa_1 = M_1$  and  $\kappa_2 = M_2$ , we obtain

$$\begin{aligned} \phi &= a_0 \left( \frac{\tau}{\tau_0} \right)^{-\left(\frac{2m}{3}\right)} \sec h^2 \eta, \\ \eta &= \left( \frac{a_0 M_1}{12 R_2} \right)^{1/2} \left( \frac{\tau}{\tau_0} \right)^{-\left(\frac{m}{3}\right)} \left\{ \xi \right. \\ &\quad \left. - \left( \frac{a_0 M_1 \tau_0}{3} \right) \left[ 1 \right. \right. \\ &\quad \left. \left. + \frac{3}{3-2m} \left[ \left( \frac{\tau}{\tau_0} \right)^{\left( 1 - \frac{2m}{3} \right)} - 1 \right] \right] \right\} \quad \dots (A15) \end{aligned}$$

where  $a_0$  is the amplitude of the wave.

**References**

- 1 Nakamura Y & Sugai H, *Chaos Solit Fractals*, 7 (1996) 1023.
- 2 Tagare S, *Plasma Phys*, 15 (1973) 1247.
- 3 Das G C & Nag A, *Phys Plasmas*, 13 (2006) 082303.
- 4 Paul S N, Chattopadhyaya S, Bhattacharya S K & Bera B, *PRAMANA-J Phys*, 60 (2003) 1217.
- 5 Lonngren K E, *Opt Quantum Electron*, 30 (1998) 615.
- 6 Deka M K, Adhikary N C, Misra A P, Bailung H & Nakamura Y, *Phys Plasmas*, 19 (2012) 103704.
- 7 Armstrong T P, Paonessa M T, Bell E V & Krimigis S M, *J Geophys Res*, 88 (1983) 8893.
- 8 Alexeff I & Neidigh R V, *Phys Rev*, 129 (1963) 516.
- 9 Williams D J, Mitchell D G & Christon S P, *Geophys Res Lett*, 15 (1988) 303.

- 10 Qureshi M N S, Shah H A, Murtaza G, Schwartz S J & Mahmood F, *Phys Plasmas*, 11 (2004) 3819.
- 11 Tribeche M & Bacha M, *Phys Plasmas*, 17 (2010) 073701.
- 12 Franz J R, Kintner P M & Pickett J S, *Geophys Res Lett*, 25 (1998) 1277.
- 13 Williams J E, Cooney J L, Aossey D W & Lonngren K E, *Phys Rev A*, 45 (1992) 5897.
- 14 Mamun A A & Shukla P K, *Phys Plasmas*, 9 (2002) 1468.
- 15 Mamun A A & Shukla P K, *Phys Lett A*, 374 (2010) 472.
- 16 Khan S A, Mahmood S & Mirza A M, *Phys Lett A*, 372 (2008) 148.
- 17 Sabry R, Moslem W M, Shukla P K & Saleem H, *Phys Rev E*, 79 (2009) 056402.
- 18 Haq M N U, Saeed R & Shah A, *J Appl Phys*, 108 (2010) 043301.
- 19 Liu H F, Wang S Q, Li C Z, Xiang Q, Yang F Z & Liu Y, *Phys Scr*, 82 (2010) 065402.
- 20 Eslami P, Mottaghizadeh M & Pakzad H R, *Phys Scr*, 83 (2011) 065502.
- 21 Ghosh D K, Chatterjee P & Ghosh U N, *Phys Plasmas*, 19 (2012) 033703.
- 22 Ghosh U N, Ghosh D K, Chatterjee P, Bacha M & Tribeche M, *Astrophys Space Sci*, 343 (2013) 265.
- 23 Demiray H & El-Zahar E R, *Phys Plasmas*, 25 (2018) 042102.
- 24 Demiray H, *Chaos Solit Fractals* 130 (2020) 109448.
- 25 Sahu B & Roychoudhury R, *Astrophys Space Sci*, 91 (2013) 345.
- 26 Ullah S, Masood W & Siddiq M, *Contrib to Plasma Phys*, 60 (2020) 201900182.
- 27 Wang Z X, Wang X Ren L, Liu J & Liu Y, *Phys Lett A*, 339 (2005) 96.